RESEARCH PAPER

Study of energy transfer from capping agents to intrinsic vacancies/defects in passivated ZnS nanoparticles

Manoj Sharma · Sunil Kumar · O. P. Pandey

Abstract The study of energy transfer mechanism from different capping agents to intrinsic luminescent vacancy centres of zinc sulphide (ZnS) has been reported in the present work. Nanoparticles of capped and uncapped ZnS are prepared by co-precipitation reaction. These nanoparticles are sterically stabilized using organic polymers—poly vinyl pyrrolidone, 2-mercaptoethanol and thioglycerol. Monodispersed nanoparticles were observed under TEM for both capped and uncapped ZnS nanopowders. However, for uncapped ZnS nanopowders, tendency for formation of nanorod like structure exists. Size of ZnS crystallites was calculated from X-ray diffraction pattern. The primary crystallite size estimated from X-ray diffraction pattern is 1.95–2.20 nm for capped nanostructures and 2.2 nm for uncapped nanostructures. FTIR spectra were conducted to confirm capping. Zeta potential measurements have been done to check the stability of dispersed nanoparticles. Band gap measurement was done by UV–visible spectrophotometer. Excitation and emission spectra are also performed in order to compare optical properties in various samples. Increase in emission intensity and band gap has been observed by adding different capping agents in comparison to uncapped ZnS nanoparticles. The results show that in capped ZnS nanoparticles the mechanism of energy transfer from capping layer to photoluminescent vacancy centres is more pronounced.

Keywords Capping · Uncapped · Excitation · Emission · Semiconductor nanoparticles

Introduction

Semiconductor nanoparticles (NPs) exhibit unique optical properties, which are strongly governed by their size (Alivisatos et al. 1989, Kalele et al. 2006). Photoluminescence (PL) of bulk and nanocrystalline ZnS is given special attention due to its potential technological applications. PL can also be used effectively to determine the size dependent electronic structure. These quantum particles have demonstrated high luminescence efficiencies and remarkably short luminescence decay times (Bhargava 1996; Kubo et al. 2002; Gilbert et al. 2006). The PL efficiency is, however, adversely affected by the presence of intrinsic surface states. In addition, the nature of the chemical treatment can dramatically affect the emission and its kinetics without affecting the absorption spectrum. Most of the physical or chemical properties exhibited by these NPs are due to their crystallites.

M. Sharma (✉) · O. P. Pandey
School of Physics and Materials Science,
Thapar University, Patiala 147 004, Punjab, India
e-mail: manojnarad@gmail.com

S. Kumar
Department of Physics, Maharishi Markandeshwar University, Mullana, Ambala 133 203, India
e-mail: sunilkumar32@gmail.com

Further growth in their size is due to agglomeration of these crystallites to form primary particles. If this growth is not controlled, then due to Ostwald ripening and vander Waals interactions between particles, they agglomerate and settle down (Warad et al. 2005; Manzoor et al. 2004). This agglomeration can be arrested by either stabilizing them electrostatically or by inducing steric hindrance at appropriate stage(s) to achieve size selective synthesis during precipitation reaction.

Electrostatic stabilization involves the creation of an electrical double layer arising from ions adsorbed on the surface and associated counter ions that surround the particle in the dispersing media. Thus, if the electric potential associated with the double layer is sufficiently high, columbic repulsion between the particles will prevent their agglomeration. Steric hindrance can be achieved by the adsorption of large molecules such as polymers on the surface of the particles. Capping agents are used for isolating NPs from each other and nearly monodispersed NPs appear as transparent colored solutions with no precipitate formation. Lyophobic (having no affinity for a solvent colloidal) particles are known to attract each other by vander Waals forces. The attraction is strong due to the near additivity of forces between pairs of unit cells in different particles. Colloids remain stable with respect to aggregation only if there exists a repulsive force of sufficient strength within the range to counteract the van der Waals attraction (Warad et al. 2005; Dongjin et al. 2006). Therefore, an ideal capping molecule should form a strong bond with the NP surface to remain attached almost permanently without interfering in any of the processes occurring inside the NPs. A proper capping passivates the surface (reduces its reactivity) and prevents the coalescence of NPs.

Normally, the emission characteristics shift to higher energy with decreasing size of NPs. The excitation tracks the absorbance, resulting in a tunable fluorophore that can be excited efficiently at any wavelength shorter than the emission peak (Denzler et al. 1998; Murase et al. 1999; Murray and Kagan 2000; Kumbhojkar et al. 2000; Manzoor et al. 2004). It will yet emit with the same characteristic of narrow, symmetric spectrum regardless of the excitation wavelength. As there is large stoke shift in case of quantum dots, their excitation wavelengths can be shifted to shorter wavelengths

for the same emission wavelength. These characteristics make QD's ideal for multicolour experiments because a whole range of emission wavelengths that can be obtained with a single excitation wavelength (Suyver et al. 2001; Manzoor et al. 2003; Ghosh et al. 2006). In this work, we have studied the PL behaviour of ZnS NPs using different capping agents and compared our results with the published data. For this study, organic polymers poly vinyl pyrrolidone (PVP), 2-mercaptoethanol (ME) and thioglycerol (TG) were taken as capping agents and their optical and morphological characteristics were studied.

Experimental

For this study, analytical grade chemicals of Sigma–Aldrich were taken. Zinc sulphide (ZnS) NPs were synthesized by chemical precipitation method (Gilbert et al. 2006; Manzoor et al. 2003). Apart from this, ZnS were also prepared under similar conditions to compare their properties (same ratio of Zn^{2+}/S^{2-}) using three different capping agents. In the first step, 40 mL homogenous solutions of 0.5 M zinc acetate and 0.5 M sodium sulphide were prepared in distilled water separately by stirring them for half an hour. Also 2% solutions of all three capping agents used in present investigation were prepared in 40 mL distilled water separately. For the synthesis of uncapped ZnS NPs, 40 mL of 0.5 M sodium sulphide solution was added drop wise to 40 mL solution of 0.5 M zinc acetate $(Zn(CH_3COO)_2 \cdot 2H_2O)$ in aqueous medium. Solution containing ZnS NPs was stirred for half an hour using a magnetic stirrer. For the synthesis of capped ZnS NPs instead of direct addition of sodium sulphide to zinc acetate solution, 40 mL solution of 2% capping agents was added slowly in 40 mL solution of 0.5 M zinc acetate. The solution was stirred for half an hour at room temperature. Then to this reaction mixture, 40 mL solution of 0.5 M sodium sulphide was added drop wise. Soon after the addition of sodium sulphide the precipitation phenomenon occurs and concentration of precipitates increases as addition was increased. The stirring was allowed for half an hour. The capping agents PVP, TG and ME were used for avoiding the particle agglomeration. The solution containing particles were then centrifuged at 4,000 rpm for 5 min. The precipitated particles were filtered using Whatman 40 filter paper. To remove the last traces of adhered

impurities, the particles were washed several times using double distilled water. The washed particles were dried in vacuum oven at 60 °C for 24 h. For the entire study, the concentration of capping agent was fixed (2 at.%) to compare the mechanism of energy transfer in capped and uncapped ZnS NPs. Second, by capping same amount of capping agents, removal of defect states in the band gap of host ZnS was also compared.

Morphological and optical characterization

The ZnS NPs were characterized by X-ray diffraction (XRD) technique using Rigaku, model D-maxIIIC diffractometer with Cu (Kα) radiation. TEM studies were conducted using transmission electron microscope (TEM), JEOL (JEM 2000FX) operating at 200 kV. For TEM study, the powder was ultrasonicated in ethanol. A drop of this solution was dropped on carbon-coated Cu grid. Ethanol was allowed to evaporate allowing powder to remain on grid. Optical absorption spectra of the ZnS particles were recorded with a double beam UV–visible spectrophotometer (Model: Perkin Elmer Lambda 3500) in the range 200–800 nm. PL studies were done with spectrometer (Model: Perkin Elmer55) using suitable filter. For PL (excitation and emission) studies, ZnS NPs in powder form were used in equal amount. FTIR spectra have been recorded in the range of 4,000–400 cm^{-1} with Perkin Elmer Spectrum BX (2). For the zeta potential measurement, Malvern Zetasizer 2000 (UK) with a He–Ne laser was used. Zeta potential measurement was done to see surface charge and hence stability of ZnS NPs. For zeta potential measurements, all samples were prepared in deionised distilled water at a pH of 7.4 and a concentration of 1 mg/mL. The electrophoretic mobility and zeta potential were measured in the capillary electrophoresis cell by injecting 3 mL solution.

Results and discussion

The XRD pattern of synthesized capped and uncapped powder is shown in Fig. 1. All samples show three broad peaks corresponding to (111), (220) and (311) planes of ZnS. It is to be noted that, the peaks observed in the XRD patterns match well with those of the β-ZnS (cubic) as reported in the ICDD
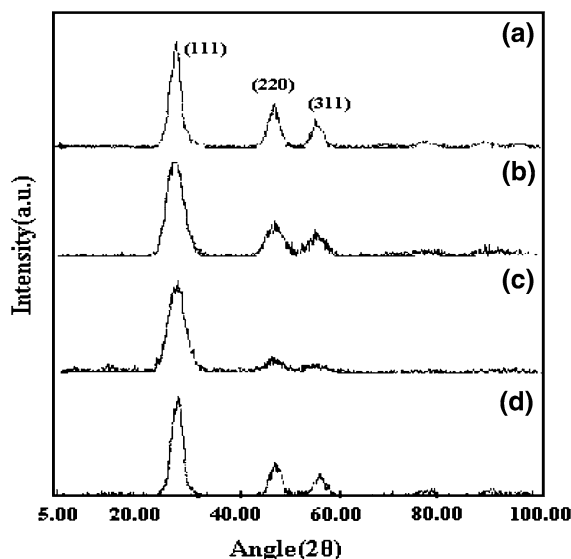

Fig. 1 XRD pattern of **a** PVP-capped, **b** TG-capped, **c** ME-capped, **d** uncapped ZnS NPs

powder diffraction file (file. No.77-2100) which appear at 2θ value of 28.5°, 47.6° and 56.4°, respectively. Broadening of the XRD peaks for both capped and uncapped samples indicates the formation of ZnS nanocrystals. The nano crystals have lesser lattice planes compared to bulk, which contributes to the broadening of peaks in the diffraction pattern. This broadening can also arise from micro straining of the crystal structure, which arises from dislocation and twinning. These defects were believed to be associated with the chemically synthesized nanocrystals as they grow spontaneously during chemical reaction since chemical species get very little time to diffuse to an energetically favourable site.

Crystallite size of ZnS NPs was calculated by following Scherrer's equation,

$$D = k\lambda/\beta\cos\theta, \tag{1}$$

where $k = 0.9$, D the crystallite size (Å), λ (Å) the wavelength of Cu (Kα) radiation and β the corrected half width of the diffraction peak. The average crystallite size calculated from these peaks using Scherrer's formula is 1.95–2.2 nm for capped ZnS NPs and 2.2 nm for uncapped ZnS NPs.

Figure 2 shows the TEM micrographs of the capped and uncapped ZnS NPs. It shows nearly monodispersed and isolated spherical crystallites,

Fig. 2 HRTEM images of **a** PVP-capped, **b** TG-capped, **c** ME-capped, **d** uncapped and **e** dark field TEM of TG-capped ZnS NPs
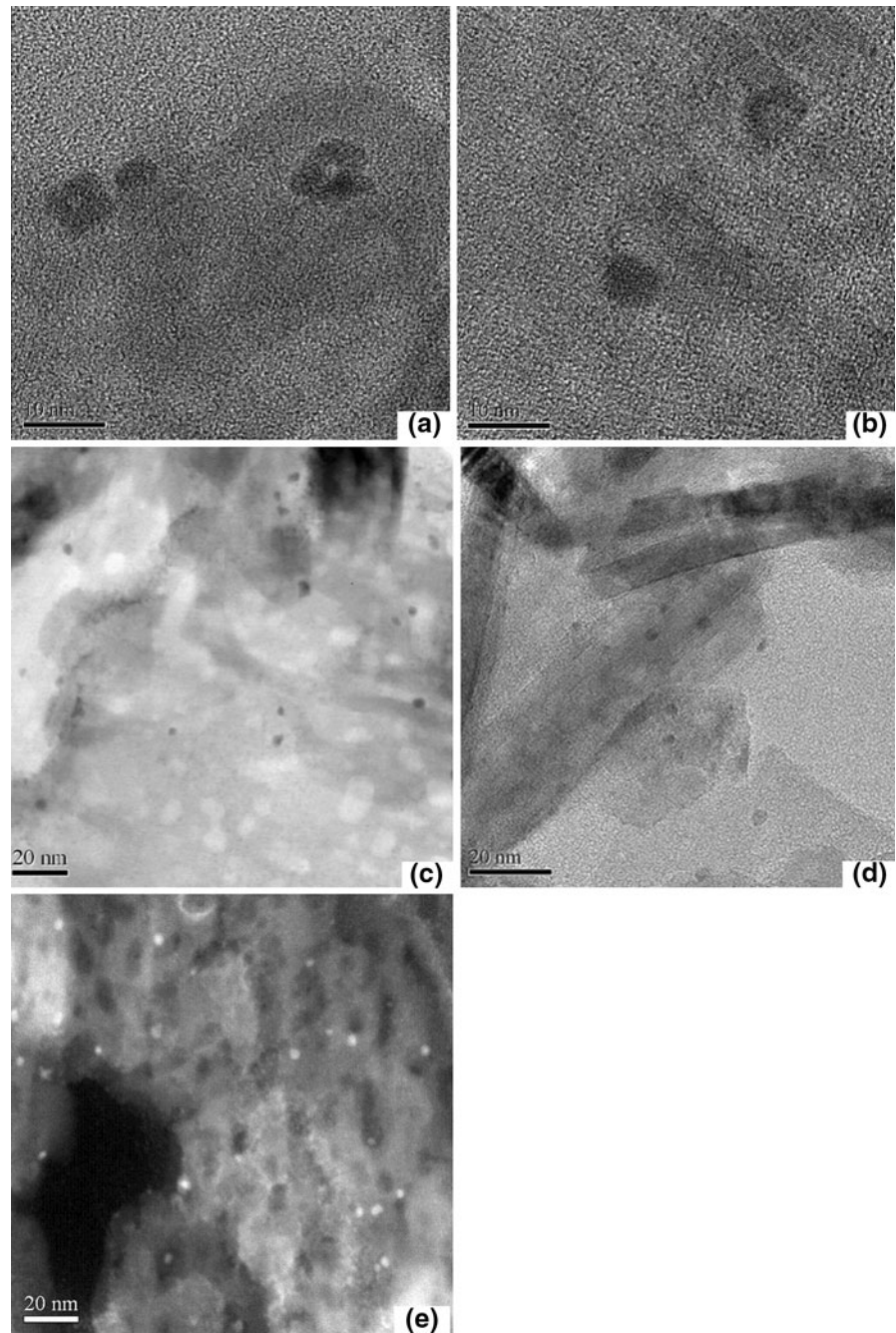
which have a mean particle size of 4 nm for capped and 5 nm for uncapped samples. Capping agents keep them isolated as can be seen in Fig. 2a, b for PVP- and TG-capped ZnS NPs. However, for ME-capped ZnS powder, little variation from spherical to angular morphology is observed. Moreover, little aggregation is also observed at some places (Fig. 2c). The NPs are

observed to be encapsulated by the capping agents. The important feature observed is the tendency for formation of nanorod like structure for uncapped ZnS powders as is evident in Fig. 2d. The diameter of nanorods is about 8–10 nm and length is 80 nm. Though this type of structure has been reported for doped ZnS with enhanced luminescence properties

Table 1 Variation of zeta potential of all samples

Sample	Zeta potential (mV)
ZnS:UC	−2.70
ZnS:PVP	−39.7
ZnS:ME	−15.7
ZnS:TG	−46.5

(Manzoor et al. 2004), but for undoped it is not reported. However, their self assembly behaviour requires a detailed study. Figure 2e shows dark field electron micrograph of TG-capped ZnS NPs. Here, quantum dots having spherical morphology can be easily distinguished.

Table 1 shows zeta potential of ZnS NPs (both capped and uncapped). In our case, capped ZnS NPs exhibit high stability as compared to uncapped ZnS NPs. TG-capped ZnS and PVP-capped ZnS NPs show relatively higher zeta potential in comparison to ME-capped and uncapped ZnS NPs.

In order to find the band gap of uncapped and capped ZnS NPs, UV–visible absorption spectra were recorded, which is given in Fig. 3. Table 2 presents the absorption edge and band gap values along with excitation wavelengths corresponding to peaks observed in Figs. 3 and 6 (discussed later), respectively. For uncapped, TG-capped, ME-capped and PVP-capped ZnS NPs, the estimated band gap values are 3.73, 3.86, 3.78 and 3.75 eV corresponding to absorption edge at 332, 321, 328 and 330 nm, respectively. It is also evident from UV–visible spectrum that there are multiple absorption peaks in each sample. Among these peaks, most predominant peak around 320 nm is due to band gap of host semiconductor and other small absorption peaks below 250 nm are assigned to ethanol in which powder samples have been dispersed for measuring the absorbance (British Pharmacopoeia 1993). FTIR spectra of all samples were recorded to know the role of different capping agent in forming bonds with ZnS NPs.

Figure 4a, b represents FTIR spectra of capped and uncapped ZnS NPs in the range of 4,000–400 cm^{-1}, whereas Fig. 5 represents the proposed interaction mechanism of different capping agents with ZnS NPs. Table 3 represents the FTIR spectra data showing the position of different groups of pure capping agents along with some observed positions in
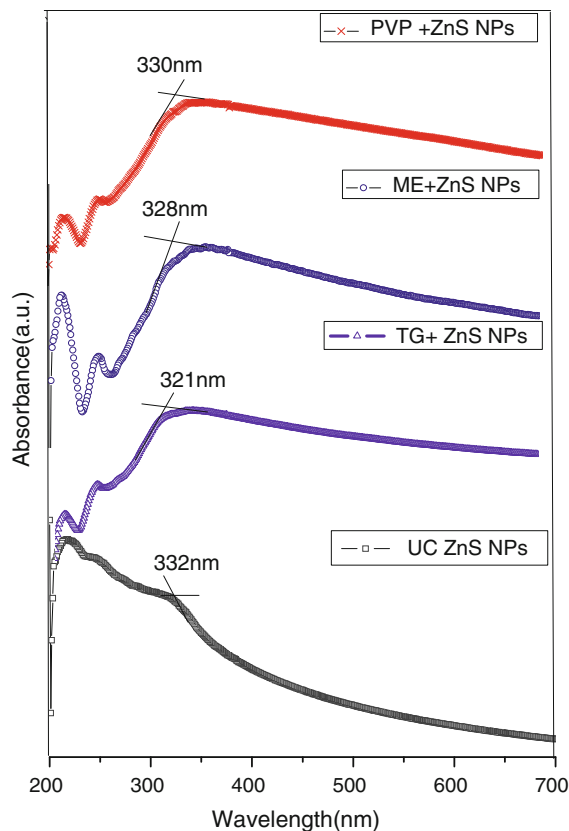

Fig. 3 UV–visible absorption spectra of **a** PVP-capped, **b** TG-capped, **c** ME-capped, **d** uncapped ZnS NPs

Table 2 Calculated band gap using absorption and excitation spectra

Sample	Absorption edge (nm) from absorption spectra	Band gap (eV) from UV–vis. Absorption spectra	Excitation (for 412 nm emission) (nm)	Band gap (eV) from excitation spectra
ZnS:UC	332	3.73	272, 300	4.50, 4.27
ZnS:PVP	330	3.75	270, 324	4.59, 3.80
ZnS:ME	328	3.78	325	3.81
ZnS:TG	321	3.86	329	3.76

our experiment for ZnS-capped NPs. The sharp peaks in all samples at 2,358 cm^{-1} is due to carbon. As shown in Table 3 and Fig. 4, the S–H vibration observed at 2,555 cm^{-1} in the pure TG and ME polymer was not observed for any of the subsequent capped ZnS sample. This gives a clear indication that the TG and ME was de-protonated and coordinated to
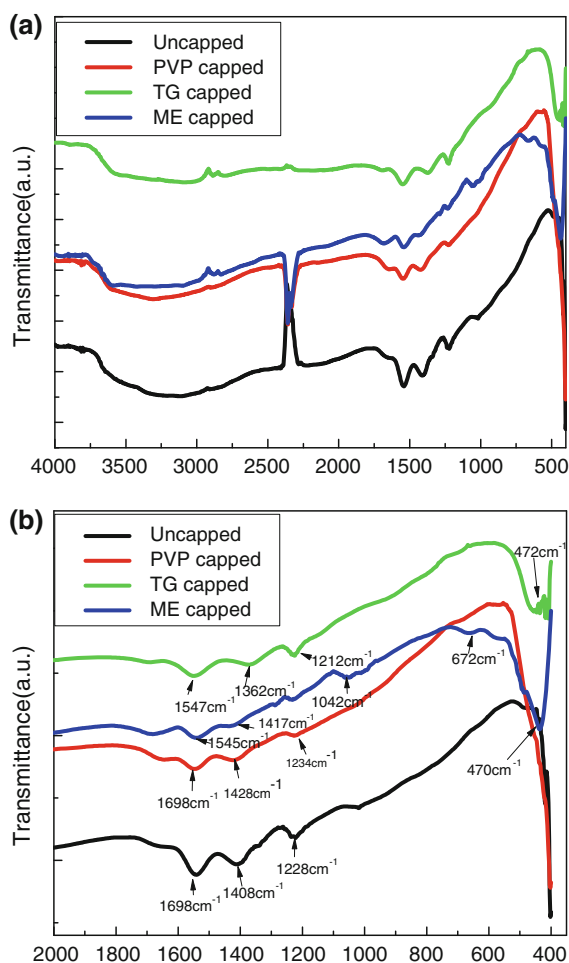
Fig. 4 a FTIR spectra of uncapped ZnS, TG-capped, PVP-capped and ME-capped ZnS, **b** magnified FTIR in the range of 2,000–400 cm^{-1}

the surface of the ZnS NPs through sulphur (Hullav-arada and Hullavarad 2008). Passivation is confirmed by the formation of S–S bond (400–600 cm^{-1}), which occurs due to breaking of S–H bonds. S–S bond arises between sulphur from thiol group existing in the capping agent and sulphur in the ZnS NPs.

Table 3 also shows (–CH$_2$–O [δs CH$_2$]) bonding, which exists from 1,470 to 1,300 cm^{-1} as reported for ME and TG polymers (Hullavarada and Hullav-arad 2008). This peak shifts to 1,362 cm^{-1} for TG-capped ZnS NPs (small intensity) and disappears for ME-capped ZnS NPs in our case. Intensity of 1417.8 cm^{-1} peak assigned to –CH$_2$–S in pure TG decreases in ME-capped ZnS sample and disappeared in TG-capped sample. The doublet of C–C stretch seen in pure sample in the region of 1,300–800 cm^{-1}
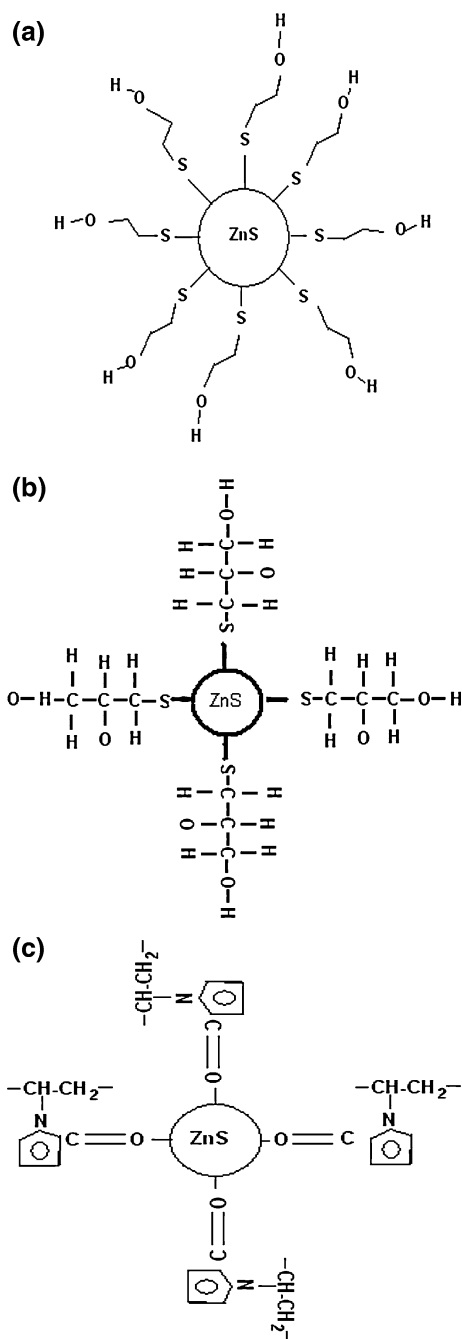

Fig. 5 Proposed capping interactions of **a** ME, **b** TG and **c** PVP with ZnS NPs

was replaced by a sharp band near 1,212 cm^{-1} in TG-capped ZnS NPs and at 1,045 cm^{-1} for ME-capped ZnS NPs. This corresponds to asymmetric stretching vibrational mode indicating a surface modification due to the passivation of ZnS NPs. This phenomenon

Table 3 The summary of results from FTIR analysis

Peak assignment	Peak position (cm^{-1})						
	PVP[a]	PVP + ZnS NPs	ME[b]	ME + ZnS NPs	TG[b]	TG + ZnS NPs	UC ZnS NPs
C–H bonding (a and s)	2,959–2,879, 1,494–1,414, 1,374	1,415	2,800–3,000	2,912, 2,838	–	2,918, 2,852, 1,362	1,404
C–O bonding	1,659, 1,295	1,551, 1,215	–	–	–	–	
O–H stretch	3,369	3,300	3,374	3,424	–		3,250
CH$_2$O [δsCH$_2$] bonding	–	–	1,470–1,300	–	1,470–1,300	1,362	–
C–C	–	–	800–1,300	1,212	800–1,300	1,045	–
CH$_2$ a (stretch)	–	–	2,930	2,912	2,930	2,918	–
S–H stretching bond	–	–	2,555.5	–	2555.5	–	–
S–S bond	–	–	–	400–600	–	400–600	–

[a] Ghosh et al. 2006, [b] Hullavarada and Hullavarad 2008 (a—asymmetric; s—symmetric)

proves the fact that ME and TG got assembled on the ZnS surface. The proposed mechanism of interaction of capping agents with ZnS NPs is shown in Fig. 6.

As given in Table 3, the peaks corresponding to C–O group reported for pure PVP at 1,659 and 1,295 cm^{-1} (Ghosh et al. 2006) shifts to 1,551 and 1,215 cm^{-1}, respectively, in our case for PVP-capped ZnS NPs. From FTIR spectra (Fig. 4a, b) of PVP-capped ZnS NPs, it is observed that there is decrease in intensity of absorption peaks followed by increase in broadness in the range 2,959–2,879 cm^{-1}; 1,374–1,548 cm^{-1}. This corresponds for coordinate bond between nitrogen of PVP with Zn^{2+} ions, which is also reported by Ghosh et al. (2006). Apart from this the peak for PVP-capped ZnS at 1,374 is due to C–H bonding (Yanagida et al. 1989; Ghosh et al. 2006). As these peaks are present in FTIR spectra of PVP, it is clear that it forms bonds with unsaturated ions on nano sized ZnS as surface to volume ratio is more in this case.

Among the capping agents used in the present investigation, it is interesting to note that both TG and ME have S–H group at one end and OH group at the other end but ME has only two C atoms chain with one OH group, whereas TG has three C atoms with two OH groups (Hullavarada and Hullavarad 2008). As the nature of capping differs drastically, it alters the size distribution (monodispersion or polydispersion) of the particles. The main difference in these three organic capping agents is the number of carbon atoms present in the molecule. In spite of these differences, when the synthesis conditions are same, all the passivating agents give rise to excitonic peak at almost the same position with ±5 nm deviation, which is confirmed from UV–visible and excitation studies (Table 2).

Thus, it is clear that in organically capped samples sulphur alone can effectively passivate ZnS in case of ME and TG, leading to the quantum size effect. The hybridization increases the localized electron density of C=O groups in PVP, S–H groups in ME and TG to promote effective energy transfer to sulphur vacancy levels, which are shown in Fig. 8(discussed later). Thus, it is evident from FTIR that, when the passivating agent encapsulates the ZnS NPs, a shift in the absorption peak is observed, indicating the process of capping being done successfully.

Figure 6 shows excitation spectra of uncapped and capped ZnS NPs for different emission wavelengths. Figure 7 presents emission spectra of uncapped and capped ZnS NPs at 272 and 325 nm excitation showing intensity comparison of various samples. Figure 8 shows emission spectra of uncapped and capped ZnS NPs at different excitation wavelengths. Figure 9 shows proposed energy band diagram for energy transfer in excitation and emission spectra.

ZnS NPs have been prepared with many stoichiometries of Zn and S. For ZnS NPs, excess Zn in ZnS gives emission in the range of 395–420 nm (Kumbhojkar et al. 2000). Excitation spectra corresponding to fixed emission in the range of 400–461 nm have been shown in Fig. 6 for uncapped and capped samples. Table 2 shows all excitation wavelengths corresponding to all possible emission sites. It also

Fig. 6 Comparison of
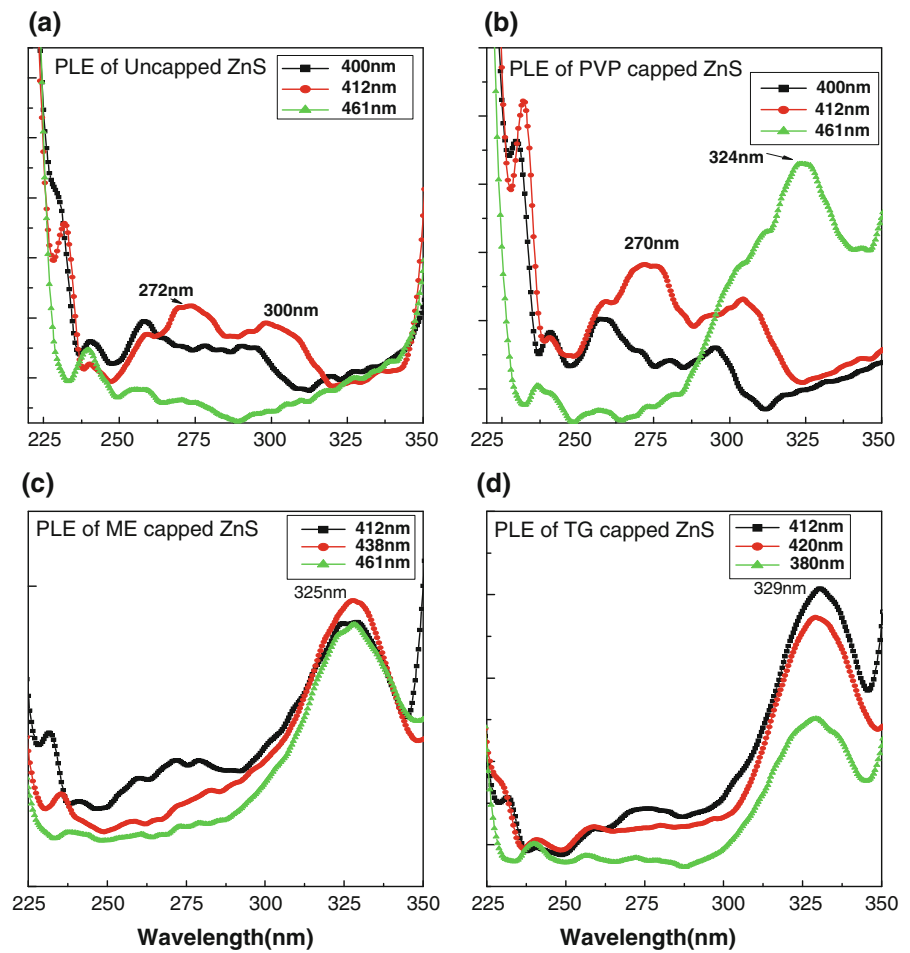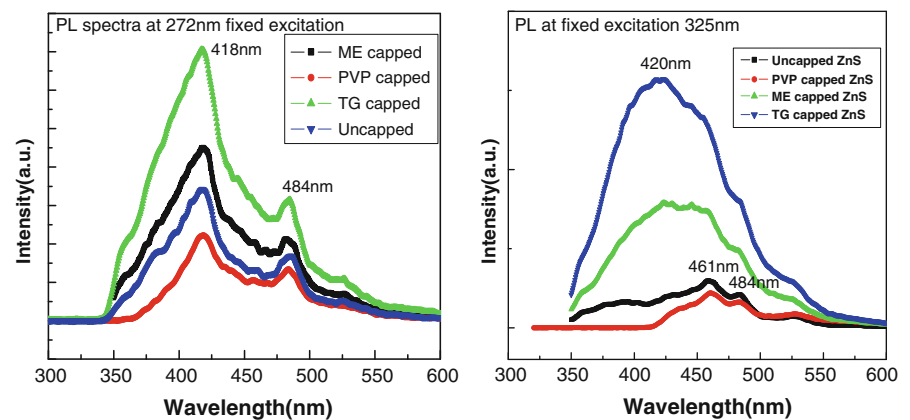excitation spectra (PLE) of
ZnS NPs

(a)

PLE of Uncapped ZnS

- 400nm
- 412nm
- 461nm

272nm   300nm

225   250   275   300   325   350

(b)

PLE of PVP capped ZnS

- 400nm
- 412nm
- 461nm

324nm

270nm

225   250   275   300   325   350

(c)

PLE of ME capped ZnS

- 412nm
- 438nm
- 461nm

325nm

225   250   275   300   325   350
Wavelength(nm)

(d)

PLE of TG capped ZnS

- 412nm
- 420nm
- 380nm

329nm

225   250   275   300   325   350
Wavelength(nm)

Fig. 7 Intensity
comparison of emission
spectra (PL) of ZnS NPs

PL spectra at 272nm fixed excitation

418nm

- ME capped
- PVP capped
- TG capped
- Uncapped

484nm

Intensity(a.u.)

300   350   400   450   500   550   600
Wavelength(nm)

PL at fixed excitation 325nm

420nm

- Uncapped ZnS
- PVP capped ZnS
- ME capped ZnS
- TG capped ZnS

461nm
484nm

Intensity(a.u.)

300   350   400   450   500   550   600
Wavelength(nm)

shows energy gap of all samples estimated from
excitation and UV–visible absorption spectra. In
Fig. 6a, excitation spectra of uncapped ZnS corre-
sponding to emission at 400, 412 and 461 nm have
been recorded, which shows weak absorptions at

multiple regions, i.e. 270 nm and 300 nm. The
excitation spectra of PVP-capped ZnS NPs shows
multiple excitation peaks corresponding to different
emission centres (Fig. 6b). Here, for emission corre-
sponding to 400 and 412 nm, the excitation spectra

Fig. 8 Comparison of emission spectra (PL) of ZnS NPs at different excitations
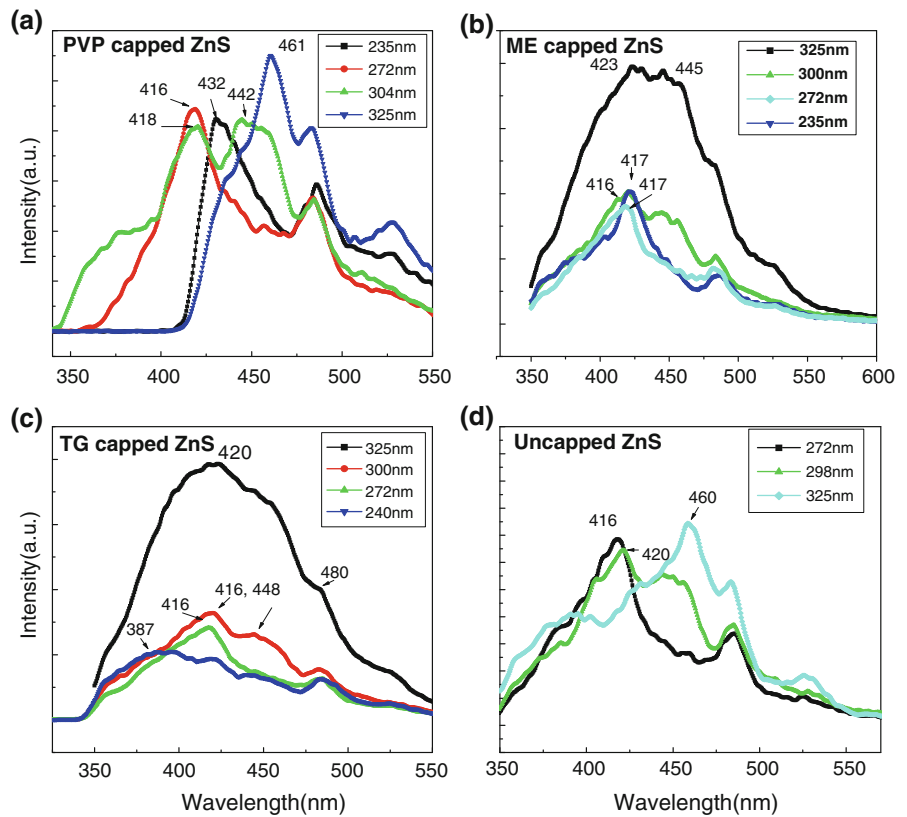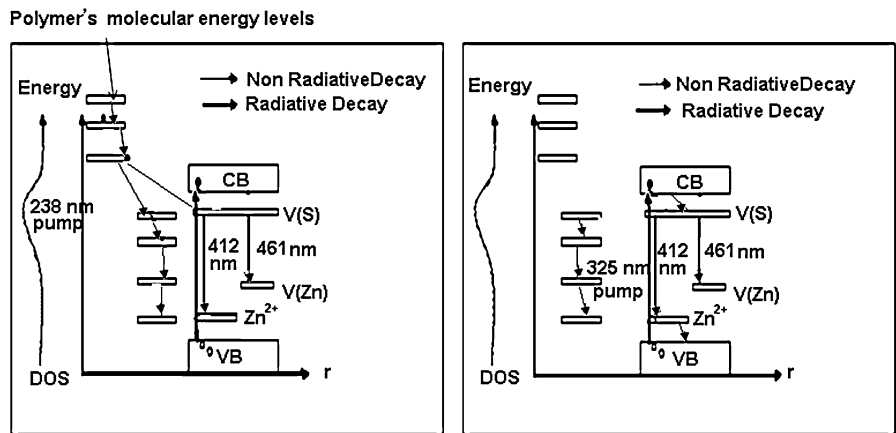

Fig. 9 Proposed energy level diagram of excitation (238 and 325 nm) and emission spectra in capped as well as uncapped ZnS NPs. *DOS* density of states, *VB* valence band, *CB* conduction band, *V(Zn)* zinc vacancy, *V(S)* sulphur vacancy)

shows small multiple peaks at 235, 270 and 295 nm. Excitation peaks at 235 and 270 nm corresponds to energy levels of PVP, which has been reported earlier by Manzoor et al. 2004, whereas excitonic peak at 295 nm can be designated for band to band excitation. However, for emission at 461 nm, excitation peak having maximum intensity shift from 270 to 325 nm. This observation indicates that higher

excitation energy (4.59 eV) is required for 400 nm emission as compared to lower excitation energy of 3.81 eV, which is required for 461 nm emission. As excitation energy (4.59 eV) corresponding to 400 nm emission is higher than the band gap of ZnS (3.81 eV), 400–420 nm emission can be due to transfer of energy from molecular energy levels of PVP to sulphur vacancies, which is further explained

by emission spectra of PVP-capped ZnS in Fig. 8a. Figure 6c shows excitation spectra of ME-capped ZnS NPs. It shows excitonic peak at 329 nm with small peak at 275 nm. Figure 6d shows TG-capped ZnS NPs having excitonic peak at 329 nm. The absorption energies corresponding to these excitation peaks are calculated and given in Table 2, which are in close agreement with those estimated by UV–visible absorption spectra. This small variation can be attributed due to multiple excitations in all samples, which are showing excitations in band to band, band to defects and band to polymer energy levels in some cases.

Yanagida et al. (1989) have observed longer wavelength defect luminescence at about 420 nm in addition to the band gap luminescence in ZnS NPs. It is well reported that emission due to sulphur vacancies is at 420 nm (Kumbhojkar et al. 2000; Suyver et al. 2001). However, with excess sulphur, these vacancies are filled; so there is quenching effect in emission of 420 nm (Suyver et al. 2001). However, at low concentration of sulphide ions during precipitation of ZnS, energy levels of large number of sulphur vacancies (Vs) are formed, which lies just below the conduction band. These vacancies are doubly ionized donor centres. Sulphur vacancies act as electron traps, whereas zinc vacancies, excess sulphur, excess zinc act as hole traps, which lie just above valence band (Suyver et al. 2001). Also impurity centres if added can act as hole traps. Due to this, electron hole recombination at the acceptor centres will lead to sulphur vacancy-related multiple emissions in case of undoped ZnS NPs.

In Fig. 7, we have shown comparison of emission intensity for all four samples at 272 and 325 nm excitations. It is clearly observed from the PL spectra that emission intensity of TG- and ME-capped ZnS NPs is high in comparison to PVP-capped and uncapped ZnS NPs. This is due to better passivation of surface defects in ME- and TG-capped ZnS NPs in

comparison to PVP-capped ZnS NPs. In uncapped ZnS, it can be due to surface defects, which causes non-radiative decay, and hence, PL intensity is less. However, in PVP-capped ZnS NPs this decrease in PL intensity can be due to various reasons. One of the reasons can be due to excess polymer adsorbed on the surface of ZnS NPs, which is weakly emissive (Manzoor et al. 2004). During emission, discrete molecular energy levels of PVP will add to non radiative decay, because PVP has its own energy levels, which have been explained earlier in the discussion of UV absorption and excitation spectra. The decrease in emission intensity for PVP-capped and uncapped ZnS NPs are observed to be similar for all other excitation wavelengths.

Figure 8 shows emission spectra of all samples at different excitation wavelengths. Table 4 shows emission peaks corresponding to all excitations. These excitation wavelengths other than band gap of host ZnS are further analyzed to understand tunable characteristics with change in excitation wavelength, which depends upon interaction of capping agents with host ZnS. Emission peak at 412 nm in all samples can be due to emission from sulphur vacancy to valence band. The increase in intensity of this peak around 412 nm in comparison to other peaks at 438 and 461 nm can be assigned for the role of capping agents. First capping agents (ME and TG) are adsorbed on surface of ZnS by making bonds with excess zinc or sulphur, which are acting as defects. These exhibit two types of intensity variation. First, a decrease in emission intensity at 438 and 461 nm is observed, which is mainly due to transfer of electron from sulphur to zinc defect states. Also, as shown in FTIR spectra that sulphur of ZnS has interacted with sulphur of ME and TG, effective capping in these cases has reduced unreacted zinc and sulphur ions, which are normally responsible for emission at 438 and 460 nm region. Second, in our samples, excess sulphur is not taken, so probability of sulphur vacancies is more. It is well reported by

Table 4 Emission spectra (having maximum intensity) of different samples at different excitations

Sample	Excitation wavelength (nm)	Emission wavelength (nm) (max.)
ZnS:UC	272, 298, 325	416, 420, 460
ZnS:PVP	235, 272, 304, 329	432, 416, (418, 442), 460
ZnS:ME	236, 272, 300, 329	417, 416, 417, (423, 445)
ZnS:TG	240, 272, 300, 325	387, 416, (416, 448), (420, 487)

Manzoor et al. (2003, 2004) that excited state life time of 420 nm emission is less in comparison to other transitions, so this can also be the reason of increased emission intensity of peak at 412 nm in all the samples in comparison to other peaks. However, in PVP-capped and uncapped ZnS NPs, these emission sites are present, which indicate a lack of effective passivation of defect states. However, PVP-capped ZnS NPs exhibit tunable emission with change in excitation wavelength. In our case, this tunable emission is excitation modulated and not size or dopant modulated (Denzler et al. 1998; Zewei et al. 2009).

For PVP-capped ZnS NPs, it is observed that if the excitation wavelength is changed from 325 to 272 nm and 235 nm on lower side, there is shift in emission peak from 461 to 400 nm (Fig. 8a). This can be explained on the similar lines that PVP has its own energy levels as explained in excitation spectra of PVP-capped ZnS NPs. So, if we excite host ZnS then it shows its own emission mechanism and if PVP molecular energy levels are excited, then emission mechanism would be different. However, in case of TG- and ME-capped ZnS NPs, there is one emission peak at 412 nm at all excitations, which shows that they are not having any energy levels of their own along with band gap of host ZnS (Fig. 8b, c). Manzoor et al. (2004) have shown energy transfer from polymer layer to dopant centres. However, in our case, tunable emission is observed from 400 to 460 nm at different excitation wavelengths. It is found that transfer of energy takes place from capping layers to energy levels of zinc states (native or defect related) and host ZnS to sulphur vacancies in all samples. From these studies, it is understood that if the emission site is fixed as in our case then capping agents or host can directly transfer energy to defect sites(interstitial or vacancies).

Manzoor et al. (2004) and Ghosh et al. (2006) have also shown an increase in PL intensity of capped ZnS NPs in comparison to uncapped ZnS NPs. However, to the best of our knowledge no one has reported tunable emission with change in excitation wavelengths as observed for PVP-capped ZnS in Figs. 6b and 8a. A detailed study is further required for optimization of capping concentration with S^{2-}/Zn^{2+} ratio, both for efficient energy transfer from capping layer to sulphur vacancies and suitable bonding of adsorbed polymer with excess unsaturated ions.

Conclusions

ZnS nanocrystals have been synthesized using chemical precipitation method. Optical and morphological measurements on ZnS nanoclusters have been carried out to investigate the effect of capping on ZnS NPs. XRD results show the variation in crystallite size from 1.95 to 2.5 nm depending upon the peaks. It is clear from the TEM studies that capped ZnS NPs avoid agglomeration in comparison to uncapped ZnS NPs. Band gap of capped ZnS NPs is found to increase in comparison with uncapped ZnS NPs indicating quantum size effects. The band gap values from UV–visible absorption and excitation studies are in correlation with each other. Increase of intensity in case of capped ZnS compared to uncapped ZnS shows that energy transfer mechanism from capping layer to photoluminescent defect centres is more pronounced. It also shows that defect-related emission in ME- and TG-capped ZnS is less in comparison to PVP-capped and uncapped ZnS NPs. In conclusion, both in TG and ME, defect states (Zn^{2+} and S^{2-}) were better passivated in comparison to PVP-capped and uncapped ZnS nanostructures.

References

Alivisatos AP, Harris TD, Carroll PJ, Stiegerwald ML, Brus LE (1989) Electron-vibration coupling in semiconductor clusters studied by resonance Raman spectroscopy. J Chem Phys 90:3463–3468

Bhargava RN (1996) Spectroscopy of isolated and assembled semiconductor nanocrystals special issue. J Lumin 70: 85–94

British Pharmacopoeia (1993) Appendix IIB, A88-A89. HMSO, London

Denzler D, Olschewski M, Sattlera K (1998) Luminescence studies of localized gap states in colloidal ZnS nanocrystals. J Appl Phys 84(5):2841–2845

Dongjin K, Min K-D, Lee J, Park JH, Chun JH (2006) Influences of surface capping on particle size and optical characteristics of ZnS:Cu nanocrystals. Mater Sci Eng B 131:13–17

Ghosh G, Naskar MK, Patra A, Chatterjee M (2006) Synthesis and characterization of PVP-encapsulated ZnS nanoparticles. J Opt Mater 28:1047–1053

Gilbert B, Huang F, Lin Z, Goodell C, Zhang H, Banfield JF (2006) Surface chemistry controls crystallinity of ZnS nanoparticles. Nano Lett 6(4):605–610

Hullavarada NV, Hullavarad SS (2008) Optical properties of organic and inorganic capped CdS nanoparticles and the effects of x-ray irradiation on organic capped CdS nanoparticles. J Vac Sci Technol A 26:1050–1057

Kalele S, Gosavi SW, Urban J, Kulkarni SK (2006) Nanoshell particles: synthesis, properties and applications. Curr Sci 91(8):1038–1052

Kubo T, Isobe T, Senna M (2002) Enhancement of photoluminescence of ZnS:Mn nanocrystals modified by surfactants with phosphate or carboxyl groups via a reverse micelle method. J Lumin 99:39–45

Kumbhojkar N, Nikesh VV, Kshirsagar A (2000) Photophysical properties of ZnS nanoclusters. J Appl Phys 88(11):6260–6264

Manzoor K, Vadera SR, Kumar N, Kutty TRN (2003) Synthesis and photoluminescent properties of ZnS nanocrystals doped with copper and halogen. Mater Chem Phys 82:718–725

Manzoor K, Vadera SR, Kumar N, Kutty TRN (2004) Energy transfer from organic surface adsorbate-polyvinyl pyrrolidone molecules to luminescent centers in ZnS nanocrystals. Solid State Commun 129:469–473

Murase N, Hirata K, Yazawa T, Kushida T (1999) Fluorescence and EPR characteristics of Mn^{2+}-doped ZnS nanocrystals prepared by aqueous colloidal method. J Phys Chem B 103:754–760

Murray CB, Kagan CR (2000) Synthesis and characterization of monodisperse nanocrystals and close-packed nanocrystal assemblies. Annu Rev Mater Sci 30:545–610

Suyver JF, Wuister SF, Kelly JJ, Meijerink A (2001) Synthesis and photoluminescence of nanocrystalline $ZnS:Mn^{2+}$. Nano Lett 1:429–433

Warad HC, Ghosh SC, Hemtanon B, Thanachayanont C, Dutta J (2005) Luminescent nanoparticles of Mn doped ZnS passivated with sodium hexametaphosphate. Sci Technol Adv Mater 6:296–301

Yanagida S, Ishimaru Y, Miyake Y, Shiragami T, Pac C, Hashimoto K, Sakata T (1989) J Phys Chem 93:2576–2582

Zewei Q et al (2009) Multicolor tuning of manganese-doped ZnS colloidal nanocrystals. Langmuir 25:10259–10262